Measurement of circular dichroism in rotationally resolved photoelectron angular distributions following the photoionization of NO $A\ ^2\Sigma^+$

David J. Leahy,[a] Katharine L. Reid,[b] Hongkun Park, and Richard N. Zare
Department of Chemistry, Stanford University, Stanford, California 94305

(Received 18 May 1992; accepted 26 June 1992)

The photoionization process NO $A\ ^2\Sigma^+$ $(v=0, N=22) \rightarrow NO^+ X\ ^1\Sigma^+$ $(v^+=0, N^+)+e^-$ is studied with sufficient photoelectron energy resolution that the photoelectron angular distributions (PADs) associated with individual rotational levels N^+ of the ion are determined. By ionizing with left and right circularly polarized light and observing the change in the rotationally resolved PADs, we can deduce all dynamical information, including the *signs* of the relative phase shifts of the photoelectron partial waves. This information constitutes the first complete description of the photoionization of a molecule. We discuss the consistency of our dynamical parameters with the Rydberg series of NO. We present a general formalism for $(1+1')$ resonance-enhanced multiphoton ionization (REMPI) PADs for rotationally resolved ion states using linearly polarized light for excitation and elliptically polarized light for ionization. Based on the dynamical parameters determined from our fit, we use this formalism to predict the total system state, i.e., three-dimensional PADs and polarization of ion rotational levels following photoionization.

I. INTRODUCTION

Photoelectron angular distributions (PADs) have long been used as a means of probing atomic photoionization dynamics.[1] The appropriate use of light polarization allows us to deduce the cross sections for each partial wave contributing to the photoionization and the phases between these partial waves. For photoionization of an atom from the state $|nl'\rangle$, spherical symmetry and the dipole approximation limit the photoelectron angular momentum l to the two values $l'-1$ and $l'+1$. In this case, the cross sections of $\sigma_{l=l'\pm1}$ for the accessible partial waves and the relative phase shift δ between these partial waves provide a *complete description*[2] of the photoionization process. This complete description must include the "sign" of the relative phase shift (i.e., δ must be distinguished from $2\pi-\delta$); this sign can be determined only when the experimental geometry imposes a "handedness" on the observations. This requirement for handedness may be satisfied by using helical light to cause photoionization.

For molecular photoionization, the task of performing a complete experiment is more challenging. The internal degrees of freedom of molecules (vibration and rotation) create a much higher density of states, both above and below the ionization potential. Because the ionization dynamics depend on the nature of the ionizing transition (especially on the change in angular momentum states), quantum-state-specific observations are desirable. Indeed, a complete description of the photoionization process cannot be obtained without this specificity. We employ the method of $(1+1')$ resonance-enhanced multiphoton ionization (REMPI) to prepare a single rovibrational level for photoionization. The use of two different frequencies of light for the excitation and ionization steps permits the formation of photoelectrons with low kinetic energies (0.1–0.2 eV). Time-of-flight photoelectron spectroscopy of these slow electrons yields an energy resolution of 2.5 meV (20 cm^{-1}). This resolution is sufficient to resolve ion rotational levels for the photoionization process NO $A\ ^2\Sigma^+$ $(v=0, N=22) \rightarrow NO^+ X\ ^1\Sigma^+$ $(v^+=0, N^+)$. Here, v and N denote the vibrational and rotational levels, respectively; the superscript + refers to the ion. The earliest "state-to-state" photoionization studies of this system were published by Reilly and co-workers.[3] Müller-Dethlefs and coworkers have studied the photoionization of NO with very high photoelectron energy resolution, using a threshold photoionization method [zero-electron kinetic energy (ZEKE)].[4] However, the quantitativeness of this method is somewhat hampered by the effects of rotational autoionization[5] and by a limited capacity for angular resolution.[6]

A further advantage of the $(1+1')$ REMPI method is control over the angular momentum alignment of the intermediate state. This alignment helps us selectively position the molecular axis with respect to the polarization vector of the ionizing light beam. Because molecules lack spherical symmetry, many photoelectron partial waves can contribute to the photoionization process—the atomic selection rule $(\Delta l=l'\pm1)$ no longer applies and the degeneracy of the molecular frame l sublevels is broken. We restrict our discussion to the case of cylindrically symmetric (i.e., linear) molecules; here, each l wave has $(2l+1)$ distinct λ components, where λ is the projection of l on the internuclear axis. Thus, a relatively large number of scattering parameters need to be determined. To perform an adequate fit to the experimental results, we need a large number of independent observables. To satisfy this requirement, we have measured rotationally resolved photoelectron angular distributions at a number of different laser polarization geometries, taking the fullest advantage of the angular momentum alignment.

[a]Present address: Department of Chemistry, University of California, Berkeley, CA 94720.
[b]Present address: Department of Chemistry, University of Nottingham, Nottingham, NG7 2R0, U.K.

 0021-9606/92/194948-10$006.00

In our previous experiments,[7,8] both the excitation and ionization light beams were linearly polarized, and we varied the angle Θ_T between their polarization vectors. Expanding on a short publication,[9] we report new results complementary to our earlier work. Here, the ionizing light is circularly polarized, and we have measured the difference in the angle-resolved photoelectron flux that results from photoionization with left and right circularly polarized light[10] as we rotate the linearly polarized excitation vector. This method is known as circular dichroism in photoelectron angular distributions (CDAD)[11] and was first applied to molecular photoionization by Appling *et al.* [12–14] The CDAD spectra yield information on the handedness of the photoionization process. Our observations provide a single-valued best fit to the relative phases $\delta_{l\lambda-l'\lambda'}$ between the asymptotic partial waves $|l\lambda\rangle$ and $|l'\lambda'\rangle$. In contrast, our earlier work[7,8] was not sensitive to the sign of the relative phases, and the best fit was double valued in $\delta_{l\lambda-l'\lambda'}$.

In Sec. II A, we present a general formalism for PADs following $(1+1')$ REMPI. The theory is specific to the case in which the excitation light beam is linearly polarized, the counterpropagating ionization light beam is elliptically polarized, and both the intermediate and ion electronic states have Σ symmetry. The equations apply to rotationally resolved PADs. This formalism is easily specialized to the limiting cases of linear or circular polarization. In Sec. II B, we extend the discussion of a "coherent control" experiment proposed by Asaro, Brumer, and Shapiro[15] to experiments involving sequential absorption of photons from two independently polarizable light beams. In Sec. III, we describe our experiment. In Sec. IV A, we present our experimental results for the system NO $A\,^2\Sigma^+(v=0,\ N=22)\rightarrow NO^+\ X\,^1\Sigma^+\ (v^+=0,\ N^+)+e^-$. The CDAD spectra are compared with the rotationally unresolved results of Appling *et al.*[13] We perform a nonlinear least-squares fit of the data to equations presented in Sec. II A to deduce the magnitudes and phases of the dipole matrix elements that connect the NO $A\,^2\Sigma^+$ state to the partial waves that describe the ionization continuum. In this fit, we simultaneously consider the linear polarization data of Allendorf *et al.*[7] In Sec. IV B, we discuss the resulting dynamical parameters generated by the fit and compare them with the theoretical predictions of Rudolph and McKoy.[16] In Sec. IV C, we discuss in more detail the meaning of a complete experiment in the context of molecular photoionization. Last, we use our dynamical parameters to predict both the three-dimensional photoelectron angular distributions and the ion angular momentum polarization (alignment and orientation) for specific final rotational levels.

II. THEORETICAL DEVELOPMENT

A. Photoionization using elliptically polarized light

In this section, we present expressions for the angular distributions of photoelectrons following $(1+1')$ REMPI in which the intermediate and ion electronic states have Σ symmetry, the excitation laser is linearly polarized, and the ionization laser is elliptically polarized. We use essentially the same formalism we have before,[17] which relies heavily on the work of Dixit and McKoy.[18] At the end of this section, we specialize the equations to the situation where the ionizing laser is circularly polarized, i.e., we present equations specific to the experiment presented in this paper.

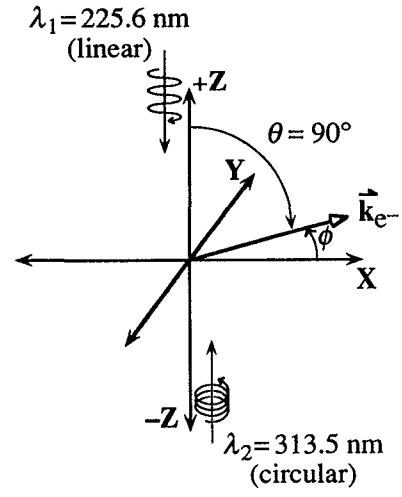

FIG. 1. A diagram of the experimental geometry. The light beams propagate along the Z axis. The detector lies in the XY plane ($\theta=90°$).

We define the laboratory Z axis to lie along the counterpropagating excitation and ionization light beams (Fig. 1). We will refer to this reference frame as the "propagation frame." The $+Z$ direction is the direction of propagation of the ionizing light beam. The X axis is chosen to lie along the linear polarization vector of the excitation light beam. The distribution of M_N sublevels prepared by the excitation is described by the density matrix elements $\rho_{M_N M_N'}$ [see Eqs. (7)–(9) of Ref. 17]; with our choice of frame, the density matrix elements are real.

We then consider ionizing this distribution of M_N sublevels with elliptically polarized light that has a propagation vector parallel (or antiparallel) to that of the exciting light. Using a semiclassical description, we write the elliptical polarization vector as a superposition of left and right circularly polarized light

$$\hat{\mathbf{e}}_{\text{ellipt}}=(E_{+1}^2+E_{-1}^2)^{-1/2}[E_{+1}\exp(i\alpha_{+1})\hat{\mathbf{e}}_{+1}+E_{-1}\exp(i\alpha_{-1})\hat{\mathbf{e}}_{-1}], \tag{1}$$

where

$$\hat{\mathbf{e}}_{+1}=\hat{\mathbf{e}}_{\text{left}}=\frac{1}{\sqrt{2}}(\hat{\mathbf{e}}_X+i\hat{\mathbf{e}}_Y) \tag{2}$$

and

$$\hat{\mathbf{e}}_{-1}=\hat{\mathbf{e}}_{\text{right}}=\frac{1}{\sqrt{2}}(\hat{\mathbf{e}}_X-i\hat{\mathbf{e}}_Y) \tag{3}$$

are the unit polarization vectors for left and right circularly polarized light, respectively. The amplitudes E_{μ_0} control the degree of elliptical polarization—if $E_{-1}=E_{+1}$, then the

light is linearly polarized; if either E_{-1} or E_{+1} is zero, then the light is circularly polarized. The phase difference $(\alpha_{-1}-\alpha_{+1})$ controls the orientation of the major axis of the ellipse. This axis lies in the XY plane (see Fig. 1) at an angle α to the X axis, where

$$\alpha=\frac{(\alpha_{-1}-\alpha_{+1})}{2}-\frac{\pi}{2}. \tag{4}$$

In general, the intensity of photoelectrons in the solid angle described by $\sin\theta\, d\theta\, d\phi$, where θ and ϕ are the polar angles, is given by

$$I(\theta,\phi)=\sum_{LM}\beta_{LM}Y_{LM}(\theta,\phi). \tag{5}$$

Here, $Y_{LM}(\theta,\phi)$ are spherical harmonics and the values of the β_{LM} coefficients depend on the photoionization dynamics, the density matrix, and the angular momentum coupling. Within the electric dipole approximation, the maximum value of L is $2n$, where n is the number of photons involved in the excitation–ionization process. Conservation of parity constrains L to take even values. In general, M can take all integral values from $-L$ to L, although the range of M is limited by the symmetry of the light polarization in the chosen frame. Note that in our previous work,[17] we chose the polarization vector of the linearly polarized ionizing light to be the quantization axis (we denote this frame as RLZ). To transform the β_{LM} coefficients of Eq. (5) from the propagation frame into the RLZ frame, we must rotate the PADs through the Euler angles $(\alpha, \pi/2, \pi/2)$, where α is defined in Eq. (4). Thus

$$\beta^{RLZ}_{LM'}=\sum_{M}D^{L}_{MM'}\left(\alpha,\frac{\pi}{2},\frac{\pi}{2}\right)\beta_{LM}, \tag{6}$$

where $\beta^{RLZ}_{LM'}$ are the coefficients in the frame of Ref. 17.

For the purposes of this paper, we are interested in the ϕ dependence of Eq. (5). The explicit form of this azimuthal dependence is as follows:

$$I(\theta,\phi)=\sum_{L}\beta_{L0}Y_{L0}(\theta,0)+\sum_{L,M\neq 0}Y_{LM}(\theta,0)\times[\mathrm{Re}(\beta_{LM})\cos M\phi-\mathrm{Im}(\beta_{LM})\sin M\phi]. \tag{7}$$

For circularly polarized light, this expression reduces to Eq. (2) of Ref. 9. The β_{LM} coefficients can be related to the magnitude $r_{l\lambda}$ and the phase $\eta_{l\lambda}$ of the dipole matrix element connecting the intermediate state to a given photoelectron partial wave $|l\lambda\rangle$,[17,18]

$$\mathrm{Re}(\beta_{LM})=\sum_{ll'}\sum_{\lambda\lambda'}\sum_{\mu_0\mu_0'}\xi_{LMl\lambda\mu_0 l'\lambda'\mu_0'}r_{l\lambda}r_{l'\lambda'}\times[\cos(\alpha_{\mu_0-\mu_0'})\cos(\eta_{l\lambda}-\eta_{l'\lambda'})-\sin(\alpha_{\mu_0-\mu_0'})\sin(\eta_{l\lambda}-\eta_{l'\lambda'})] \tag{8a}$$

$$=\sum_{ll'}\sum_{\lambda\lambda'}\sum_{\mu_0\mu_0'}\xi_{LMl\lambda\mu_0 l'\lambda'\mu_0'}r_{l\lambda}r_{l'\lambda'}\times\cos(\alpha_{\mu_0-\mu_0'}+\delta_{l\lambda-l'\lambda'}) \tag{8b}$$

and

$$\mathrm{Im}(\beta_{LM})=\sum_{ll'}\sum_{\lambda\lambda'}\sum_{\mu_0\mu_0'}\xi_{LMl\lambda\mu_0 l'\lambda'\mu_0'}r_{l\lambda}r_{l'\lambda'}\times[\cos(\alpha_{\mu_0}-\alpha_{\mu_0'})\sin(\eta_{l\lambda}-\eta_{l'\lambda'})+\sin(\alpha_{\mu_0}-\alpha_{\mu_0'})\cos(\eta_{l\lambda}-\eta_{l'\lambda'})] \tag{9a}$$

$$=\sum_{ll'}\sum_{\lambda\lambda'}\sum_{\mu_0\mu_0'}\xi_{LMl\lambda\mu_0 l'\lambda'\mu_0'}r_{l\lambda}r_{l'\lambda'}\times\sin(\alpha_{\mu_0-\mu_0'}+\delta_{l\lambda-l'\lambda'}), \tag{9b}$$

where $\mu_0=\pm 1$ is the projection of the ionizing photon angular momentum on the laser propagation axis, $\alpha_{\mu_0-\mu_0'}=\alpha_{\mu_0}-\alpha_{\mu_0'}$, and $\delta_{l\lambda-l'\lambda'}=\eta_{l\lambda}-\eta_{l'\lambda'}$. The $\xi_{LMl\lambda\mu_0 l'\lambda'\mu_0'}$ coefficients contain the density matrix and the angular momentum coupling and are specific to a value of N^+. These coefficients are related to the $\gamma_{N^+l\lambda m_l l'\lambda' m_l'}(\Theta_T)$ coefficients in Eq. (15) of Ref. 17 as follows:

$$\xi_{LMl\lambda\mu_0 l'\lambda'\mu_0'}=\sum_{m_l m_l'}(-1)^{m_l}E_{\mu_0}E_{\mu_0'}\left[\frac{(2l+1)(2l'+1)(2L+1)}{4\pi}\right]^{1/2}\times\begin{pmatrix} l & l' & L\\ m_l & -m_l' & M\end{pmatrix}\begin{pmatrix} l & l' & L\\ 0 & 0 & 0\end{pmatrix}\times\gamma_{N^+l\lambda m_l l'\lambda' m_l'}(\Theta_T=90^\circ), \tag{10}$$

where the appropriate values for μ_0 and μ_0' must be inserted into Eq. (13) in Ref. 17. We note that, due to a typographical error, the factor $(-1)^{m_l}$ was omitted from Eqs. (6) and (17) in Ref. 17.

The expressions for the β_{LM} coefficients above can be specialized to the cases of linearly or circularly polarized ionizing light by using the appropriate values of α_{μ_0} and E_{μ_0} in Eqs. (8), (9), and (10). For linearly polarized light, only the first term of Eq. (8a) and the second term of Eq. (9a) contribute, and the intensity is dependent on the cosine of the phase differences between partial waves $\delta_{l\lambda-l'\lambda'}$.:

$$\beta_{LM}=\sum_{ll'}\sum_{\lambda\lambda'}\sum_{\mu_0\mu_0'}\xi_{LMl\lambda\mu_0 l'\lambda'\mu_0'}r_{l\lambda}r_{l'\lambda'}\cos\delta_{l\lambda-l'\lambda'}\times(\cos\alpha_{\mu_0-\mu_0'}+i\sin\alpha_{\mu_0-\mu_0'}). \tag{11}$$

When PADs of this form are observed, analysis yields double-valued results for the relative phases because $\delta_{l\lambda-l'\lambda'}$ is indistinguishable from $2\pi-\delta_{l\lambda-l'\lambda'}$. Comparison of Eq. (11) with Eq. (6) in Ref. 17 reveals that, for

linearly polarized light, a simpler expression results if the polarization vector is chosen as the quantization axis.

For circularly polarized light, only the first term of Eq. (8a) and the first term of Eq. (9a) contribute to the sums, and the photoelectron intensity is sensitive to the handedness of the photoionization process through the dependence on the sine of the phase differences between partial waves

$$\beta_{LM}=\sum_{ll'}\sum_{\lambda\lambda'}\xi_{LMl\lambda\mu_0 l'\lambda'\mu_0}r_{l\lambda}r_{l'\lambda'}(\cos\delta_{l\lambda-l'\lambda'} +i\sin\delta_{l\lambda-l'\lambda'}). \quad (12)$$

Here, the sum over μ_0 and μ_0' has been collapsed because, in the propagation frame, μ_0 takes only one value when the light is circularly polarized. In addition, M is restricted to the values 0 and ± 2, and the imaginary term of Eq. (12) makes a nonzero contribution only when $L=2$ and $M=\pm 2$.

In this paper, we are particularly interested in the difference in intensity that results from photoionization with left and right circularly polarized light at each angle ϕ, i.e., the CDAD signal. In our experimental CDAD geometry, the detector is in the XY plane (see Fig. 1) and so the angle θ is fixed at 90°. Using Eqs. (7) and (12), we can write the CDAD intensity for each ion rotational state as

$$\begin{aligned} I_{\mathrm{CDAD}}(\phi)&\equiv I_{\mathrm{left}}(\phi)-I_{\mathrm{right}}(\phi)\\ &=I(\theta=90°,\phi,\mu_0=+1)-I(\theta=90°,\phi,\mu_0=-1)\\ &=\sqrt{\frac{15}{2\pi}}\mathrm{Im}(\beta_{22})\sin 2\phi, \end{aligned} \quad (13)$$

where $\mathrm{Im}(\beta_{22})$ must be evaluated for $\mu_0=-1$, i.e., $E_{+1}=0$ and $E_{-1}=1$. We note that for a given partial wave, the maximum $\Delta N(\equiv N^+-N)$ for which CDAD occurs is given by $|\Delta N|_{\max}=l-1$. In our calculations, this result is independent of the dynamical parameters $r_{l\lambda}$ and $\delta_{l\lambda-l'\lambda'}$.

B. "Coherent control"

In 1988, Asaro, Brumer, and Shapiro[15] proposed that the *angle-resolved* branching ratio in a photofragmentation process could be controlled by varying the polarization of a single light beam acting on a J, M-selected state. In their scheme, this polarization is equivalent to controlling the phase relation between two beams of light, one left circularly polarized and the other right circularly polarized. This coherent control is a quantum mechanical interference effect in which the dissociation level can be reached by more than one pathway; in this case, the two pathways correspond to absorption of left or right circularly polarized light. Our experiments can be regarded as a variation of this concept. Absorption of one photon establishes a certain amount of M selection in a molecular ensemble. A second photon, with independently controllable polarization, interacts with this M-selected ensemble. The two light beams do not have a coherent phase relationship, but the memory of the first photon remains in the polarization of the molecular ensemble, and this polarization can lead to quantum interferences. We have reported modest control over the *angle-integrated* rotational branching ratios following the photoionization of NO (see, e.g., Table V of Ref. 8). For this system, the extrema of the angle-integrated branching ratios are realized by using *linear* polarization geometries—the $\Delta N\neq 0$ transitions are minimized for $\Theta_T=0°$ and maximized for $\Theta_T=90°$. Thus, our experiments demonstrate quantum interference effects that can be controlled and manipulated by the experimentalist, and as such are an example of coherent control.

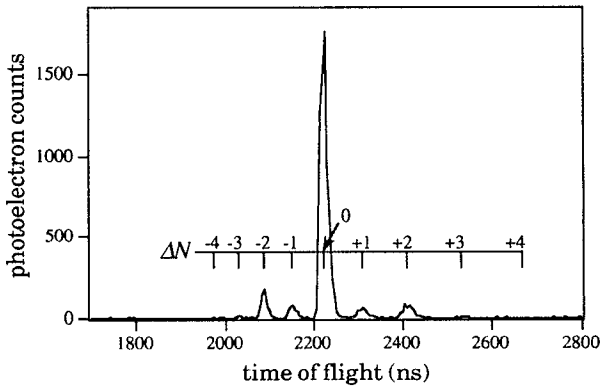

FIG. 2. The time-of-flight photoelectron spectrum of the $(1+1')$ photoionization process NO $X\,^2\Pi(v=0,\ J=22.5)\rightarrow A\,^2\Sigma^+(v=0,\ N=22)\rightarrow NO^+\,X\,^1\Sigma^+(v^+=0,\ N^+)+e^-$. The full width at half-maximum (FWHM) of each peak is 2.5 meV.

III. EXPERIMENT

The photoelectron spectrometer has been described previously.[7,8] The excitation light beam was tuned to resonance with the $X\,^2\Pi(v=0)\rightarrow A\,^2\Sigma^+(v=0,\ N=22)\ P_{21}+Q_1(22.5)$ transition of NO at 225.6 nm. The ionization light beam was tuned to 313.5 nm, matching the wavelength used by Allendorf *et al.*[7] in their linear polarization study of the same system. Unlike in our earlier work, both lasers were unfocused. The energies of the excitation and ionization light beams were 500 nJ/pulse and 100 μJ/pulse, respectively. A careful study of photoelectron signal vs excitation and ionization laser power showed that no detectable saturation of either step was present under these conditions (see Ref. 19 for a discussion of saturation effects for this system). We note that partial saturation of either step will reduce the effective anisotropy of the process and cause a decrease in magnitude of the CDAD signal. A typical photoelectron time-of-flight spectrum is shown in Fig. 2. An especially high signal-to-background ratio allowed us to observe the very weak $\Delta N=\pm 3$ transitions in this experiment. Over the range of kinetic energies measured in this experiment (from 136 meV for $\Delta N=+3$ to 203 meV for $\Delta N=-3$), the detection efficiency of the experiment was not constant owing to the effect of small stray electric fields generated by nonuniform surface potentials of the drift tube. A linear detection efficiency parameter was included in the data analysis to correct this artifact; the resulting correction modified the intensities of the $\Delta N=\pm 2$ peaks by $\pm 10\%$, respectively.

Circularly polarized light was prepared by passing linearly polarized light at 314 nm through a zero-order quarter-waveplate centered at 314 nm (Special Optics) at normal incidence. The quarter-waveplate was rotated such that its optic axes formed 45° angles with the plane of polarization. The handedness of the outgoing light beam depends on the relative orientation of the "net fast axis" of the quarter-waveplate and the plane of polarization. To determine the handedness of the light (and thus to determine which of the two optic axes of the quarter-waveplate was "fast"), we analyzed the beam with a single Fresnel rhomb (Karl Lambrecht), exploiting the well-characterized behavior of the phase shifts on total internal reflection.[20] In other words, we knew which "axis" of the rhomb was fast and we used this knowledge to assign the fast and slow axes of the quarter-waveplate. When properly oriented, the rhomb restored the circular polarization to linear; the direction of this linear polarization revealed whether the input beam had left- or right-handed helicity.

With this knowledge of the sense of helicity, we recorded photoelectron angular distributions for both left and right circularly polarized light. These measurements were made by rotating the plane of polarization of the linearly polarized excitation beam with a zero-order half-waveplate. As before, our time-of-flight spectrometer gave an energy resolution of $\sim$2.5 meV, sufficient to resolve single rotational levels of NO^+ for values of $N^+ \geqslant 10$. The rotationally resolved time-of-flight spectra were recorded at nine angles spanning 180° for each helicity of the ionization beam. Details of our data acquisition method are given in Refs. 7 and 9. For this experiment, we accumulated data for 25 000 laser shots at each angle. This effort resulted in approximately 2200 counts per angle for the strong $\Delta N(\equiv N^+ - N) = 0$ transition, approximately 150 counts per angle in the weaker $\Delta N = \pm 1$ and ± 2 transitions, and perhaps eight counts per angle for the $\Delta N = \pm 3$ transitions.

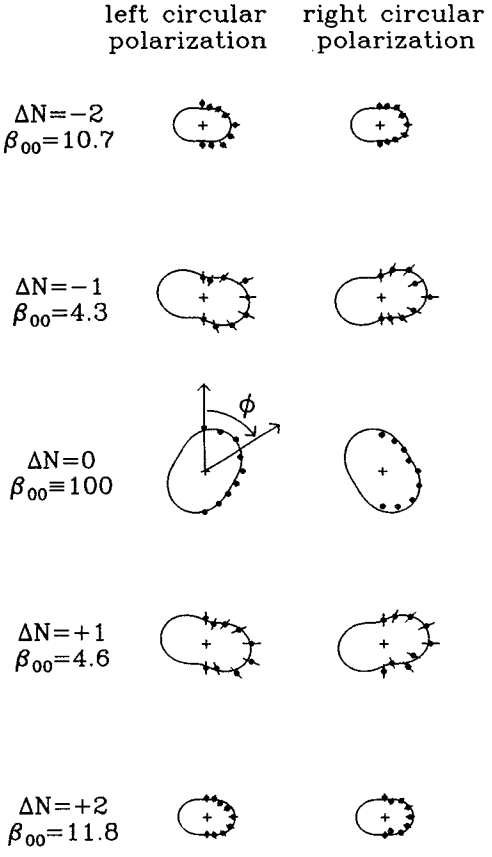

FIG. 3. Polar plots of the experimental photoelectron angular distributions (PADs) for five ion rotational levels. The plots are scaled to uniform size; the angle-integrated cross sections β_{00} are listed on the left. The ϕ dependence is depicted in the $\Delta N = 0$ left circular polarization plot. The error bars represent 2σ uncertainties. The solid lines are the predictions of the model based on the results of the fit shown in Table I.

IV. RESULTS AND DISCUSSION

A. Experimental results and fit to dynamical parameters

In Fig. 3, we show the polar plots of the experimental PADs that result from photoionization with left and right circularly polarized light for each ion rotational state denoted by $\Delta N = N^+ - N$. In Fig. 4, we replot these results on Cartesian axes along with the CDAD spectrum for each ΔN. We can immediately see a significant CDAD signal for $\Delta N = 0$ and $\Delta N = \pm 1$, but very little for $\Delta N = \pm 2$. Furthermore, we observe that the sign of the CDAD spectrum for $\Delta N = 0$ is opposite to that of the $\Delta N = \pm 1$ transitions. This result is significant because the selection rule[21] $\Delta N + l$ = odd is good for Σ–Σ transitions. The rotational resolution permits independent observation of $\delta_{l\lambda - l'\lambda'}$ contributions for the even l waves (s and d, with $l = 0$ and 2, respectively) and the odd l waves (p and f, with $l = 1$ and 3).

As in our earlier work,[7,8] we have chosen a $P_{21} + Q_1$ transition for the excitation. This transition has mostly Q character (P:Q is about 1:8 for the transitions we have studied) and provides the highest degree of alignment available to us for the higher values of N. Because the size of the CDAD signal is proportional to the degree of alignments,[11] this choice maximizes the CDAD signal. White and co-workers have previously observed the rotationally unresolved CDAD spectra of NO for various branches.[13] The transition most similar to our study was $P_{21} + Q_1(16.5)$. They quote the coefficient of $\sin 2\phi$ in this CDAD spectrum [see Eq. (13)] to be -0.104 ± 0.005 for this transition, normalized to the PAD intensity at $\phi = 90°$.[13] They also calculate (by *ab initio* methods) the rotationally summed CDAD coefficient to be -0.206. The coefficient we obtain when we rotationally sum our CDAD spectra and normalize to the PAD intensity at $\phi = 90°$ is $+0.204 \pm 0.012$, which is essentially the same in magnitude as the theroretical calculation of Ref. 13. The difference in N value does not account for the large discrepancy between the magnitude of the experimentally determined CDAD coefficient given in Ref. 13 and that found in this study (the sign of the CDAD spectrum is discussed below). The most likely explanation is that Appling *et al.*[13] partially saturated the optical transitions. We note that the excita-

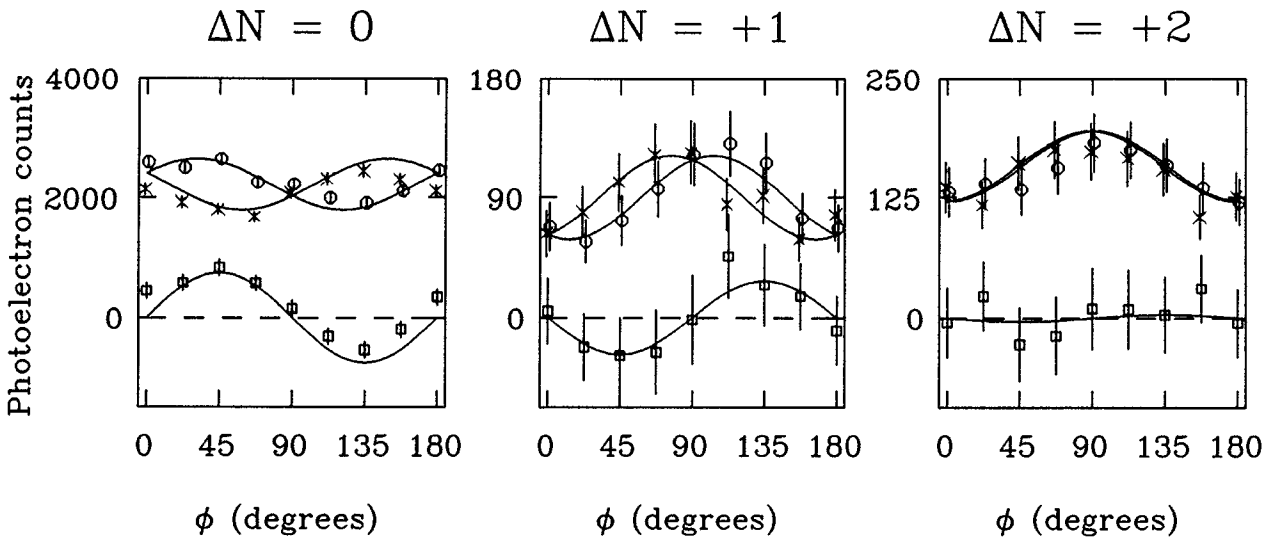

FIG. 4. Cartesian plots of the PADs and the CDAD spectra for three ion rotational levels. The Y axes indicate the number of electrons observed at each angle. The circles denote the signal from ionizing with left circular light; the x's, from right circularly polarized light; and the squares are the difference signal $I_{\mathrm{CDAD}}(\phi)$. The error bars represent 2σ uncertainties. The solid lines are the predictions of the model based on the results of the fit shown in Table I.

tion light beam used by Appling *et al.* was 1000 times more intense than that used in our experiment.

Analysis of the experimental data required close attention to established conventions regarding the definition of left- and right-handed light. The angular momentum of left circularly polarized light is taken to point parallel to the propagation vector, while that of right circularly polarized light points antiparallel.[22] In quantum mechanical terms, this means simply that for right circularly polarized light, $\mu_0=-1$. Classically, right circularly polarized light, when viewed toward the source of the light beam, has its electric vector revolve in a clockwise sense as time moves forward. Thus, right circularly polarized light has the phase of the $\hat{\mathbf{e}}_X$ component 90° ahead of the $\hat{\mathbf{e}}_Y$ component [see Eq. (3)]. The experimental determination of the ionizing light beam's helicity is discussed in Sec. III. Our choice of phases for rotational wave functions, described in Ref. 17, follows that of Zare.[23] By expressing our formalism in the propagation frame, we have avoided rotating the frame of the circularly polarized photon, an operation that would cause a helicity change depending on whether the rotation is considered in the "active" or "passive" sense.[24,25] It is this frame rotation that makes a direct comparison of the sign of our CDAD spectra with the rotationally summed predictions of Appling *et al.*[13] difficult. We assume that the choice of reference frame is what gives rise to the sign discrepancy between our measurement and the theoretical prediction in Ref. 13.

The best way of comparing our results with theoretical predictions is to fit our experimental data to extract the dynamical parameters $r_{l\lambda}$ and $\delta_{l\lambda-l'\lambda'}$ [see Eqs. (8) and (9)] and compare them with those calculated by Rudolph and McKoy.[16] To perform this fit, we use the data shown in Fig. 3, along with the PADs reported by Allendorf *et al.*[7] in which the ionization light beam was linearly polarized with $\Theta_T=0°$ and $\Theta_T=90°$. Although the transition studied in this linearly polarized work was $P_{21}+Q_1(25.5)$, one of the assumptions of the model is that the photoionization dynamics are independent of the rotational level ionized. We have reanalyzed our earlier data[7] to include data for all transitions with $|\Delta N|\leqslant 4$ in our fit. Although the signal-to-noise ratio for the $\Delta N=\pm 3$ and ± 4 transitions was low (the signal was actually zero for ± 4), this inclusion improved considerably the quality of the fit for the d and f waves. The ion rotational resolution is essential for us to obtain a unique fit to all of the dynamical parameters. We fit the linearly polarized data to Eqs. (7) and (11) and the circularly polarized data to Eqs. (7) and (12) using calculated values for the ξ parameters.

The dynamical parameters $r_{l\lambda}$ and $\delta_{l\lambda-l'\lambda'}$ that result from the fit are presented in Table I. As discussed in Ref. 8, the partial wave expansion of the photoelectron wave function has been truncated at $l=3$. We see that the dynamical parameters have been well determined and that the signs of the phase differences $\delta_{l\lambda-l'\lambda'}$ have been deduced. To clarify our discussion, we present the phases over the interval $(-180°, 180°)$, as opposed to the more conventional interval $(0°,360°)$. The parameters listed in Table I (together with the total ionization cross section, measured by Zacharias, Schmiedl, and Welge[26] to be 7.0×10^{-19} cm^2) constitute a complete description of this molecular photoionization process (see Sec. IV C).

The PADs predicted by the results of the fit are shown as solid lines in Figs. 3 and 4. We find the fit to be satisfactory; the statistical uncertainties of the data represent the vast majority of the error for all but the $\Delta N=0$ transitions. For this transition, the statistical error bars are relatively small, and some residual systematic error (perhaps up to 5% of the intensity) is visible. We attribute the systematic error to small deviations from ideal polarization

TABLE I. Parameters resulting from the fit of experimental data for photoionization of NO via the $A\,^2\Sigma^+$ ($v=0$) state. Also shown are the results of the *ab initio* calculation of Rudolph and McKoy (Ref. 16). The $r_{l\lambda}$ values are normalized so that their squares sum to unity. The total ionization cross section [$\sigma=7.0(9)\times10^{-19}$ cm^2] has been measured by Zacharias, Schmiedl, and Welge (Ref. 26). The values in parentheses represent 1σ uncertainties. Other relative phases (e.g., $\delta_{d\pi-s\sigma}$) can be calculated easily from the values listed here.

Parameter	Fit[a]	*Ab initio*[b]
$r_{s\sigma}$	0.204(2)	0.158
$r_{p\sigma}$	0.503(11)	0.278
$r_{p\pi}$	0.471(6)	0.537
$r_{d\sigma}$	0.166(30)	0.221
$r_{d\pi}$	0.073(15)	0.020
$r_{f\sigma}$	0.321(25)	0.358
$r_{f\pi}$	0.244(13)	0.268
$\delta_{p\pi-p\sigma}$	+12.4°(1.5)	+9.9°
$\delta_{d\pi-d\sigma}$	−68°(13)	−92.8°
$\delta_{f\pi-f\sigma}$	−1°(18)	−1.6°
$\delta_{d\sigma-s\sigma}$	−157°(9)	+173.7°
$\delta_{f\sigma-p\sigma}$	−59°(14)	−76.3°

[a]The relative phases in Ref. 8 included the phase factor of i^l. Thus, the definition of $\delta_{d\sigma-s\sigma}$ and $\delta_{f\sigma-p\sigma}$ differs from that of Ref. 8 by 180°.
[b]The phase factors of i^l and $(-1)^\lambda$ have been removed from the phases given in Ref. 16.

quality of the two light beams and to minor beam path deviations that arise from the rotation of the waveplates.

B. Dynamical interpretation and comparison with *ab initio* results

Our interpretation of the photoionization dynamics for the system NO $A\,^2\Sigma^+ \rightarrow NO^+ X\,^1\Sigma^+ + e^-$ remains essentially unchanged.[7,8] The photoionization cross section is dominated by the contribution of the p wave, which shows little preference for parallel or perpendicular character. This interpretation agrees well with the description of the NO $A\,^2\Sigma^+$ state as an s Rydberg state. We see sufficient f wave in the photoionization to indicate that the NO^+ ion potential has a significant quadrupolar moment. The small partial cross sections for the s and d waves suggest that the dipole moment of the potential must be relatively weak. Because our results agree so well with the *ab initio* calculations of Rudolph and McKoy (see below),[16] the one-electron picture seems adequate to describe the direct photoionization of the NO $A^2\Sigma^+$ state.

The new information on circular dichroism obtained from this experiment is the observation of contributions from terms that are proportional to $\sin\delta_{l\lambda-l'\lambda'}$ [see Eq. (12)]. The results of the fit are better determined as a result of this additional observation. Perhaps more significant is that the overall fit no longer has double-valued relative phase shifts $\delta_{l\lambda-l'\lambda'}$. The physical interpretation of the phase shift is the relative attractiveness of the potential for the outgoing partial waves $|l\lambda\rangle$ and $|l'\lambda'\rangle$.[27] In our earlier work, we determined only the size of the relative phase shift. Our CDAD spectra have revealed which partial waves are actually attracted more strongly than the others.

An interesting parallel can be drawn between the Rydberg series of NO and our observed relative phase shifts for the transition dipole matrix elements for ionization from the $A\,^2\Sigma^+$ state. The continuity between high-lying Rydberg states and near threshold photoionization continuum states has long been recognized; this continuity is the focus of the quantum defect theory.[28] The quantum defect is known to be directly related to the scattering phase shift. Although the relative phase shifts we have deduced from our photoionization experiment are not the same as scattering phase shifts, a qualitative analogy can still be drawn between these two quantities. An obscuring detail is that, in general, molecular Rydberg states do not have good quantum numbers for l and λ; so the one-to-one correspondence between the "$nl\lambda$" Rydberg series and the asymptotic $l\lambda$ partial wave is only approximate. The Rydberg series of NO, however, are relatively unscrambled by the anisotropic ion core potential, especially in the p and f series. For this reason, the quantum numbers l and λ are fairly good for these series.

Applying these ideas to the case in hand, we consider our observation that the phase of the $p\pi(\lambda=\pm1)$ partial wave is advanced by $+12°$ with respect to that of the $p\sigma(\lambda=0)$ partial wave. The sign of this phase suggests that the $p\pi$ wave is more attracted to the ion core than the $p\sigma$ wave. This result is completely consistent with the relative stability of the $np\lambda$ Rydberg states, just below the onset of the ionization continuum. The $np\pi$ states have a larger quantum defect ($\mu_{p\pi}=0.75$) than the $np\sigma$ states ($\mu_{p\sigma}=0.66$)[29] and are correspondingly more strongly bound. The relative phase shift predicted by these quantum defects is $(\mu_{p\pi}-\mu_{p\sigma})\pi=+0.28$ rad, or $+16°$, in good agreement with our result. A similar result is found for the $f\sigma$ and $f\pi$ partial waves—our fit reveals almost no phase difference, and the Rydberg series have essentially the same quantum defect $\mu_{f\lambda}=0.03$. The agreement for the phases between the p and f partial waves is less good. Our fit reveals $\delta_{f\sigma-p\sigma}$ to be $-59°$, but the Rydberg series quantum defects give $(\mu_{f\sigma}-\mu_{p\sigma})\pi=-1.98$ rad, or $-113°$. This discrepancy arises at least in part because of the l-dependent Coulomb phase shift, which we have not included; thus our analogy is overly simplistic for the comparison of partial waves with different values of l. Last, because of the relatively mixed nature of the "s" and "d" Rydberg series,[30] we cannot easily apply these arguments to interpret the relative phases of the s and d partial waves.

In the right-hand column of Table I we list the *ab initio* dynamical parameters calculated by Rudolph and McKoy.[16] In general, there is excellent agreement, including the signs of the phase differences. We note that the $\delta_{d\pi-d\sigma}$ and $\delta_{d\sigma-s\sigma}$ relative phases do not agree within the uncertainty of the fit, but because these quantities are obtained from a relatively small amount of information, namely, the weak $\Delta N=\pm1$ and ±3 transitions, we are reluctant to draw conclusions about these discrepancies. As an alternative way of comparing their results with ours, we have calculated rotationally resolved CDAD spectra using their parameters. The results are shown in Fig. 5, scaled for comparison with the results of our fit. Although

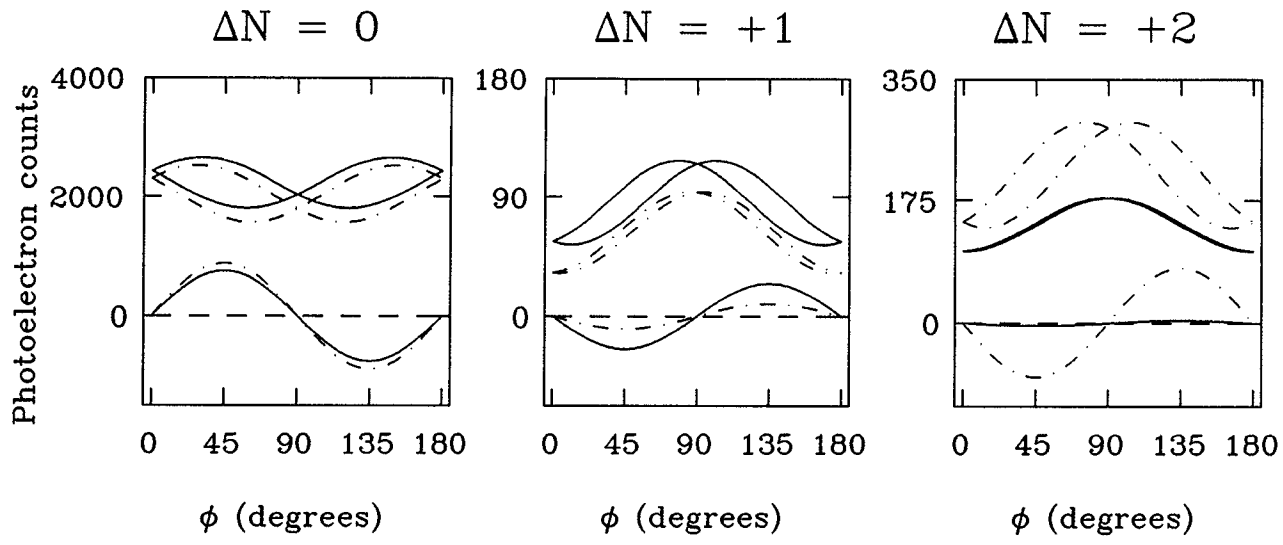

FIG. 5. A comparison of the predictions of the fit with the *ab initio* predictions of Rudolph and McKoy (Ref. 16). The solid lines were calculated using the experimentally derived parameters listed in the first column of Table I, while the dotted–dashed lines are the theoretical predictions derived from the second column. The scaling of the *ab initio* results to the results of the fit was performed such that the total photoionization cross section was equal for the two calculations.

their prediction $\Delta N=0$ CDAD signal (the major contributor to the rotationally summed signal) is in good agreement with our measurement, we see that the agreement is less good for $\Delta N=-1$ and that there is a large discrepancy for the rotational levels corresponding to $\Delta N=-2$. Although we observed almost no CDAD signal for the $\Delta N=-2$ transition, the parameters of Rudolph and McKoy predict a CDAD signal that is up to $\sim 30\%$ of the helicity-averaged signal. Also, as we have observed before,[8] there is substantial disagreement between the experimental $(\Delta N=0):(\Delta N=\pm 2)$ branching ratio and the theoretical prediction for this quantity. The reason for this discrepancy is the difference between the result of their calculated value and our fit value for the ratio $r_{p\sigma}:r_{p\pi}$, i.e., the fraction of parallel character of the p wave. In light of our results, we are quite confident that the true value for this ratio is approximately one, as opposed to their calculated value of approximately one-half.

C. Completeness in molecular photoionization

A complete (or "perfect") scattering experiment has been defined by Bederson[31] and Kessler[2] to be an experiment that permits the unique determination of all of the theoretical parameters that completely describe the process. "Completely describe" means that all the quantities of the system state that result from the process can be predicted with knowledge of these theoretical parameters. In the case of photoionization, one must be able to predict unambiguously the internal state distribution of the ion, including its alignment and orientation, the three-dimensional photoelectron angular distributions, the angle-resolved spin orientation of the photoelectron, and all possible vector correlations between these quantities. Subject to the approximations and assumptions of our formalism discussed below, the dynamical parameters $r_{l\lambda}$ and $\delta_{l\lambda-l'\lambda'}$ are sufficient to completely describe the photoionization process $NO\ A\ ^2\Sigma^+ \rightarrow NO^+\ X\ ^1\Sigma^+ + e^-$.

The assumptions we have made in deeming our experiment complete should be discussed. As is usual, we neglect the contributions of interactions of higher order than the electric dipole. We truncate the photoelectron partial wave expansion at $l=3$ (see Refs. 7 and 8) because there is no sizeable contribution from rotational transitions with $|\Delta N|>2$. We assume that the photoionization dynamics are independent of the molecular rotational level and that the photoionization dynamical parameters are constant over the range of photoelectron kinetic energies involved in our experiment (136–203 meV). The influence of nuclear and electronic spins in our system of study is very weak, although nonzero. Therefore we expect the emitted photoelectron to have negligible spin polarization. Finally, for this photoionization process (but not in all cases; see, e.g., Ref. 32), the relative phase shifts between even and odd l waves are unobservable (disregarding a measurement of the coherence between N^+ levels) and have been excluded from
Table I.

Using the dynamical parameters from the fit, we can predict the angular momentum polarization (i.e., alignment and orientation) of the molecular ion formed in each final rotational level. The procedure for doing this is explained in Sec. II C of Ref. 17. When the ionizing light is circularly polarized, the ensemble of rotational angular momentum vectors of the ion can be oriented as well as aligned. Alignment refers to the situation in which the ensemble of N vectors has the symmetry of a double-ended arrow, while orientation arises when the N vectors point preferentially in one direction like a single-ended arrow. In Fig. 6, we show the angular momentum polarization of the NO^+ ion for $N^+=22$, 23, and 24 following the excitation

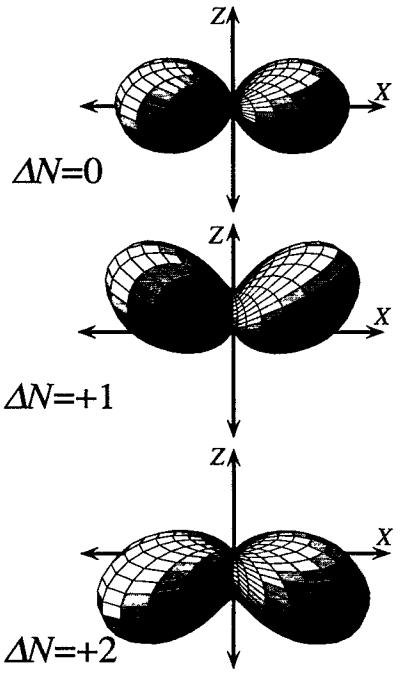

FIG. 6. Predictions of the three-dimensional distributions of the rotational angular momentum of NO^+ calculated from the results of the fit listed in Table I. The view is from a point in the YZ plane above the Y axis (not shown).

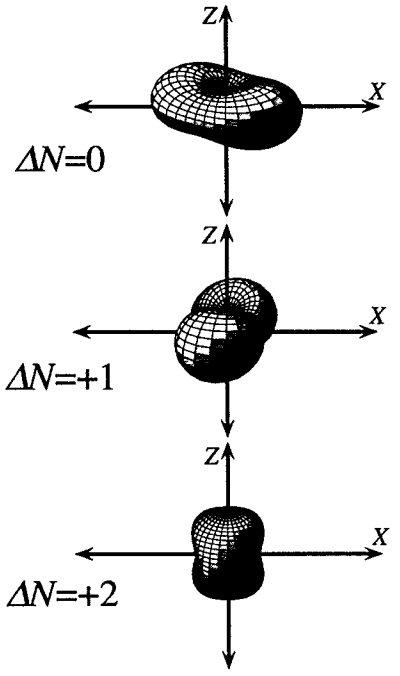

FIG. 7. Predictions of the three-dimensional PADs calculated from the results of the fit listed in Table I. The view is from a point in the YZ plane above the Y axis (not shown).

$P_{21}+Q_1(22.5)$ to the $A\,^2\Sigma^+$ state with left circularly polarized light, based on the dynamical parameters listed in Table I. Because the excitation step is essentially a Q transition, the ensemble of **N** vectors in the intermediate state lies preferentially parallel to the polarization vector, i.e., along the X axis. As in our earlier work,[8] we predict that for the $\Delta N=0$ transition, this alignment is essentially unchanged by the ionization. For the $\Delta N=+1$ transition, the ionization step favors those **N** vectors that are more nearly parallel to the propagation vector, and we see that the distribution of $\mathbf{N}^+$ vectors bends toward the $+Z$ axis, giving rise to orientation. The $\Delta N=+2$ transition causes orientation in the opposite direction. For each value of ΔN, we predict the opposite orientation for $+\Delta N$ vs $-\Delta N$ transitions; e.g., $\Delta N=-1$ would look essentially like $\Delta N=+1$, except that the orientation would be in the $-Z$ direction. This situation is exactly analogous to bound–bound transitions—P and R branches create opposite orientation upon excitation with circularly polarized light. Although the direction of orientation changes when the helicity of the light is reversed, the *shape* of the distribution of $\mathbf{N}^+$ vectors does not change. This is different from the PADs, which show no orientation, but have different shapes following photoionization with left and right circularly polarized light. In Fig. 7, we show the three-dimensional photoelectron angular distributions for the same transitions as those plotted in Fig. 6. As in Fig. 6, these PADs have been calculated by using the dynamical parameters deduced from the fit. The CDAD sin 2ϕ dependence appears in these plots as a left–right asymmetry. The direction of the skewing is seen to be opposite for the $\Delta N=0$ and $\Delta N=+1$ transitions. On the other hand, because virtually no CDAD spectrum is predicted for the $\Delta N=+2$ transition, the PAD is almost cylindrically symmetric.

V. CONCLUSIONS

We have presented the first observation of circular dichroism in photoelectron angular distributions (CDAD) for rotationally resolved ion levels. We observe that this dichroism depends on the ion rotational level and in particular note that the nonobservation of CDAD for our $\Delta N=\pm 2$ PAD is an important measure of the $p\sigma$ to $p\pi$ ratio in the photoelectron wave function. We have been able to determine the *signs* of the relative phases between photoelectron partial waves and so have probed the handedness of the photoionization process. Because our results constitute a complete description of the photoionization process $NO\ A\,^2\Sigma^+(v=0,N)\rightarrow NO^+\ X\,^1\Sigma^+(v^+=0,N^+)+e^-$, we have also predicted three-dimensional PADs and the polarization of the angular momentum of the final ion rotational levels. We have presented a formalism that is general for any degree of ellipticity of ionizing light and for any alignment of the level ionized.

ACKNOWLEDGMENTS

We thank Sham Dixit and Sarah Allendorf for helpful discussions. K.L.R. thanks the SERC for a NATO postdoctoral fellowship. We acknowledge the support of the National Science Foundation under Grant PHY 90-20457.

[1] See, e.g., H. Kaminski, J. Kessler, and K. J. Koliath, Phys. Rev. Lett. **45**, 1161 (1980); A. Hausmann, B. Kammerling, H. Kossmann, and V. Schmidt, *ibid.* **61**, 2669 (1988); U. Heinzmann, J. Phys. B **13**, 4353 (1980); U. Heinzmann, *ibid.* **13**, 4367 (1980); O. C. Mullins, R.-L. Chien, J. E. Hunter, J. S. Keller, and R. S. Berry, Phys. Rev. A **31**, 321 (1985).
[2] J. Kessler, Comments At. Mol. Phys. **10**, 47 (1981); H. Klar and H. Kleinpoppen, J. Phys. B **15**, 933 (1982).
[3] W. G. Wilson, K. S. Viswanathan, E. Sekreta, and J. P. Reilly, J. Phys. Chem. **88**, 672 (1984); K. S. Viswanathan, E. Sekreta, E. R. Davidson, and J. P. Reilly, *ibid.* **90**, 5078 (1986).
[4] K. Müller-Dethlefs, M. Sander, and E. W. Schlag, Chem. Phys. Lett. **112**, 291 (1984); M. Sander, L. A. Chewter, K. Müller-Dethlefs, and E. W. Schlag, Phys. Rev. A **36**, 4543 (1987); G. Reiser, W. Habenicht, K. Müller-Dethlefs, and E. W. Schlag, Chem. Phys. Lett. **152**, 119 (1988).
[5] See, e.g., S. T. Pratt, J. L. Dehmer, and P. M. Dehmer, J. Chem. Phys. **90**, 2201 (1989).
[6] G. Reiser, D. Rieger, and K. Müller-Dethlefs, Chem. Phys. Lett. **183**, 239 (1991).
[7] S. W. Allendorf, D. J. Leahy, D. C. Jacobs, and R. N. Zare, J. Chem. Phys. **91**, 2216 (1989).
[8] D. J. Leahy, K. L. Reid, and R. N. Zare, J. Chem. Phys. **95**, 1757 (1991).
[9] K. L. Reid, D. J. Leahy, and R. N. Zare, Phys. Rev. Lett. **68**, 3527 (1992).
[10] N. A. Cherepkov, Chem. Phys. Lett. **87**, 344 (1982).
[11] R. L. Dubs, S. N. Dixit, and V. McKoy, Phys. Rev. Lett. **54**, 1249 (1985); J. Chem. Phys. **85**, 656 (1986); **88**, 968 (1988).
[12] J. R. Appling, M. G. White, T. M. Orlando, and S. L. Anderson, J. Chem. Phys. **85**, 6803 (1986).
[13] J. R. Appling, M. G. White, R. L. Dubs, S. N. Dixit, and V. McKoy, J. Chem. Phys. **87**, 6927 (1987).
[14] J. Winniczek, R. L. Dubs, J. R. Appling, V. McKoy, and M. G. White, J. Chem. Phys. **90**, 949 (1989).
[15] C. Asaro, P. Brumer, and M. Shapiro, Phys. Rev. Lett. **60**, 1634 (1988).
[16] H. Rudolph and V. McKoy, J. Chem. Phys. **91**, 2235 (1989).
[17] K. L. Reid, D. J. Leahy, and R. N. Zare, J. Chem. Phys. **95**, 1746 (1991).
[18] S. N. Dixit and V. McKoy, J. Chem. Phys. **82**, 3546 (1985).
[19] D. C. Jacobs and R. N. Zare, J. Chem. Phys. **85**, 5457 (1986); D. C. Jacobs, R. J. Madix, and R. N. Zare, *ibid.* **85**, 5469 (1986).
[20] M. Born and E. Wolf, *Principles of Optics* (Pergamon, Oxford, 1970), p. 49.
[21] S. N. Dixit, D. L. Lynch, V. McKoy, and W. M. Huo, Phys. Rev. A **32**, 1267 (1985).
[22] E. Hecht, *Optics*, 2nd ed. (Addison-Wesley, Menlo Park, CA, 1987), p. 276.
[23] R. N. Zare, *Angular Momentum* (Wiley, New York, 1988), pp. 104–106.
[24] A. A. Wolf, Am. J. Phys. **37**, 531 (1969).
[25] R. N. Zare, Ref. 23, pp. 75–77.
[26] H. Zacharias, R. Schmiedl, and K. H. Welge, Appl. Phys. **21**, 127 (1980). In this work, photoionization was performed with 266 nm light.
[27] R. N. Zare, Ref. 23, pp. 31–32.
[28] M. J. Seaton, Proc. Phys. Soc. (London) **88**, 801 (1966); C. Greene and Ch. Jungen, Adv. At. Mol. Phys. **21**, 51 (1985) and references therein.
[29] E. Miescher, Can. J. Phys. **54**, 2074 (1976); T. Ebata, T. Imajo, N. Mikami, and M. Ito, Chem. Phys. Lett. **89**, 45 (1982); T. Ebata, Y. Anezaki, M. Fujii, N. Mikami, and M. Ito, J. Phys. Chem. **87**, 4773 (1983); J. W. J. Verschuur, J. Kimman, H. B. van Linden van den Heuvell, and M. J. van der Wiel, Chem. Phys. **103**, 359 (1986).
[30] Ch. Jungen, J. Chem. Phys. **53**, 4168 (1970).
[31] B. Bederson, Comments At. Mol. Phys. **1**, 41 (1969).
[32] D. J. Leahy, K. L. Reid, and R. N. Zare, J. Phys. Chem. **95**, 8154 (1991).